JOURNAL OF PHYSICAL ORGANIC CHEMISTRY, VOL. 8, 47–53 (1995)

REACTION OF PHENOXY RADICAL WITH NITRIC OXIDE

T. YU, A. M. MEBEL AND M. C. LIN*
Department of Chemistry, Emory University, Atlanta, Georgia 30322, U.S.A.

The association of C_6H_5O with NO was studied with the cavity-ring-down method by directly monitoring the decay of C_6H_5O in the presence of varying, excess amounts of NO. The bimolecular rate constant determined in the temperature range 297–373 K can be effectively represented by $k_1 = 10^{-12.12\pm0.24}e^{(194\pm185)/T}$ cm^3 molecule^{-1} with a negative activation energy of 0·8 kcal mol^{-1} (1 kcal = 4·184 kJ). In order to understand better the mechanism of the reaction, *ab initio* molecular orbital calculations were also carried out at the MP4(SDQ)/6–31G* level of theory using the HF optimized geometries. The molecular structures and energetics of five $C_6H_5N_1O_2$ isomers were calculated. Among them, the most likely and stable association product, phenyl nitrite (C_6H_5ONO), was found to be 17 kcal mol^{-1} below the reactants, $C_6H_5O + NO$. Combining the measured rate constant and the calculated equilibrium constant for the association reaction, $C_6H_5O + NO = C_6H_5ONO$ the rate constant for the unimolecular decomposition of C_6H_5ONO was obtained as $k_{-1} = 4·6 \times 10^{15}E^{-8580/T}$ s^{-1}. The relatively large frequency factor suggests that a loose transition state was involved in the reaction, akin to those of its alkyl analogs (RONO, R = CH_3, C_2H_5, etc.).

INTRODUCTION

The phenoxy radical, C_6H_5O, is a key intermediate in the oxidation of small aromatic hydrocarbons, which are important ingredients of lead-free gasoline.[1] Few kinetic data are available in the literature on its reactions except the unimolecular decomposition process

$$C_6H_5O \rightarrow CO + C_5H_5$$

which has been well characterized.[2–5]

The bimolecular reaction of C_6H_5O with CH_3 has been reported to produce primarily *o*- and *p*-cresols, instead of anisole,[6] because of the existence of the following resonance structures:

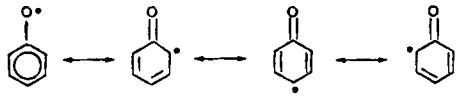

The reaction is believed to take place via vibrationally excited cyclohexadienone intermediates formed by the association of CH_3 with C_6H_5O;[7] for example,

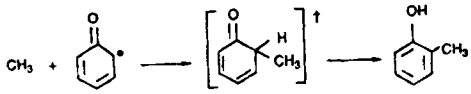

The rate-limiting H-migration process in the mechanism for the formation of *o*- and *p*-cresols is not fully understood,[8] however.

In the present study, we measured the absolute rate constant for the association of C_6H_5O with NO by the direct probing of the phenoxy radical with the cavity-ring-down (CRD) method. This novel multipass laser resonance absorption technique[9,10] was recently developed by us for kinetic–spectroscopic studies of C_6H_5 and NH_2 radical reactions.[11–15] This work represents our first study of phenoxy kinetics, carried out by monitoring the $\tilde{A} \leftarrow \tilde{X}$ transition[16] of the C_6H_5O radical in the visible region.

In order to elucidate the mechanism of the $C_6H_5O + NO$ reaction, we also performed *ab initio* molecular orbital calculations for the stability of various $C_6H_5N_1O_2$ isomers which may be formed in the association process. The results of these experimental and theoretical studies are reported herein.

EXPERIMENTAL MEASUREMENTS

Basic principle of kinetic measurement by the CRD method

The application of the CRD technique to kinetic studies of radical reactions has been described in detail previously.[11–15] This novel multipass resonance absorption technique measures the decay time of an injected pulse of photons from a tunable dye laser into a well aligned optical cavity consisting of a pair of highly reflective

* Author for correspondence

CCC 0894–3230/95/010047–07

Received 1 August 1994
Revised 22 September 1994

mirrors ($R \geq 0{\cdot}9999$). The photon decay times measured in the presence and absence of absorption, t_c and t_c^0, respectively, can be related to the concentration of the absorbing radical of interest (C_6H_5O) and other physical properties of the reaction medium according to the equation[11,12]

$$1/t = 1/t_c^0 + (cl\varepsilon/nL)[A]_t \quad (1)$$

where c is the velocity light, l is the length of the absorbing medium, ε is the extinction coefficient, n is the refractive index, L is the length of the cavity (which is 50 cm in the present case) and $[A]_t$ is the concentration of C_6H_5O at time t after its generation with a pulsed UV laser using anisole ($C_6H_5OCH_3$) as the radical source.

For a simple association process without the problem of reverse redissociation reaction, such as $C_6H_5 + NO \rightarrow C_6H_5NO$,[14] the combination of the relationship $[A]_t = [A]_0 e^{-k't}$ and equation (1) describes quantitatively the rate of C_6H_5 decay (with the pseudo-first-order constant k') measured under NO excess conditions. In the present reaction system, because of the weakness of the (C_6H_5O)—NO bonds, attached either to the O atom or to the C atoms in the ring, the reverse process of the reactions

$$C_6H_5O + NO \underset{-1}{\overset{1}{\rightleftharpoons}} (C_6H_5O)NO \quad (2)$$

becomes significant above room temperature. Accordingly, a more general rate equation which includes the reverse process should be used.

According to basic chemical kinetics, the inclusion of the reverse reaction (−1) in the rate equation (2) leads to

$$-\frac{dx}{dt} = k_1([A]_0 - x)[NO] - k_{-1}x \quad (3)$$

where $x = [A]_0 - [A]_t$ is the conversion of the C_6H_5O radical at time t into C_6H_5ONO. Integration of equation (3) under excess NO conditions gives

$$x = \frac{a}{b}(1 - e^{-bt}) \quad (4)$$

where $a = k_1$ [NO][A]$_0$ and $b = k_1[NO] + k_{-1}$. Combination of equations (1) and (4) leads to the following expression for the photon decay time measured before the photodissociation of $C_6H_5OCH_3$ (t_c^0), that measured immediately after the dissociation ($t = 0$, t_{c0}) and that measured at t after the dissociation (t_c^0):

$$1/t_c - 1/t_c^0 = ck_{-1}/b + (ck_1[NO]/b)e^{-bt} \quad (5)$$

where $c = 1/t_{c0} - 1/t_c^0$, which is constant for each individual experimental run. The results obtained by means of both equations (1) and (5) will be presented later.

Experimental set-up

The experimental arrangement of the CRD method for kinetic studies of NH_2 and C_6H_5 radical reactions has been described in detail previously.[13,15] We shall briefly mention the key components of the experimental setup here.

Two pulsed lasers were employed in the CRD study, one for the detection of the C_6H_5O radical and the other for the generation of the radical by the UV dissociation of its precursor, $C_6H_5OCH_3$. The probing tunable dye laser (Laser Photonics N_2 pumped dye laser) with a pulse width of *ca* 5 ns was injected into the reactor along its axis through one of the cavity mirrors which vacuum-sealed the reactor. The small fraction of the visible photons transmitted through the second mirror (*ca* 10^{-4} of the incident beam energy which was typically about 1 mJ per pulse) was filtered and detected with a photomultiplier (PMT) (Hamamatsu). The photoelectric signal was averaged and digitized with a LeCroy 9310 M multichannel digital oscilloscope. The averaged signal was stored and processed with a microcomputer (Genius 486). A pulse-delay generator (SRS DG535) interfaced with the computer was employed to control the delay time between the photodissociation and probing lasers. This time interval defines the chemical decay time of the C_6H_5O radical in the presence of varying, excess amounts of NO.

The photodissociation laser (Lambda Physik LPX 100 excimer laser operating at 193 nm with ArF) was split into two beams which crossed at a 15° angle at the centre of the reactor. Both the probing dye and UV dissociation lasers formed a horizontal plane which was perpendicular to the flow of reaction mixture in order to provide rapid replenishment of the sample between two dissociation laser pulses (typically 0·5 s). The flow rates of individual gases, $C_6H_5OCH_3$, NO and the carrier gas Ar, were measured with mass flow meters (Hastings and Baratron) and the total pressure of the reaction mixture was measured near the reactor with a Baratron capacitance manometer.

Reagent-grade NO and $C_6H_5OCH_3$ were purchased from Aldrich; they were purified by trap-to-trap distillation before use. In the case of NO, a clean silica gel trap maintained at 195 K was used to remove NO_2 impurity, which was always present in the commercial source of NO. The Ar carrier gas (Specialty Gases, 99·995%) was employed without further purification.

AB INITIO MO CALCULATIONS

The geometries of various structures of $C_6H_5NO_2$ have been optimized at the RHF/6–31G* level.[17] It is well known that the RHF approximation with split-valence basis sets, including polarization functions, for HNO_2 and HONO reproduces the experimental geometries or results of higher level calculations,[18] with possible

errors of 0·03–0·05/Å and 3–5° for bond distances and angles, respectively. All the isomers were positively identified for equilibrium (the number of imaginary frequencies is zero), based on vibrational frequency calculations at the RHF/6–31G* level. The calculated zero-point energy corrections (ZPE) were scaled by 0.89 to account for anharmonicity.[17] To obtain more reliable energies of the isomers of $C_6H_5NO_2$, we carried out MP4(SDQ)/6–31G* calculations at the HF optimized geometries. All calculations were performed by using the GAUSSIAN 92 program.[19] The total and relative energies of different structures are presented in Table 1.

We considered five different isomers of $C_6H_5NO_2$, **1–5**, shown in Figure 1. The isomers C_6H_5ONO (**1**), *o*-NOC_6H_5O (**2**) and *p*-NOC_6H_5O (**3**) can be obtained directly in the reaction of C_6H_5O with NO, when the NO radical attaches C_6H_5O to the oxygen atom and the *ortho*- and the *para*-carbon, respectively. Since the meta isomer of OC_6H_5O and the *m*-benzoquinone $C_6H_4O_2$ do not exist, we do not consider here the *m*-NOC_6H_5O structure, which is not expected to be a local minimum. $C_6H_5NO_2$ (**4**) can be transformed from **1** by nitrito–nitro rearrangement. The isomer **5**, $C_6H_4(OH)(NO)$, can be obtained from **2** by hydrogen shift. In the present case, however, the isomerization reactions are kinetically unlikely.

The isomer **1** lies 12·9 kcal mol^{-1} (1 kcal = 4·184 kJ) higher than the most stable structure **5** at the MP4(SDQ)//HF/6–31G* + ZPE level. C_6H_5ONO possesses C_s symmetry with the mirror plane containing the ONO group and two carbons of the ring. Aromaticity of the ring is preserved in **1** and all CC distances are similar, 1·38–1·39 Å. We calculated only the *cis*-ONO conformation of **1**, but the *trans* conformation is also expected to exist and to have the energy close to that of the *cis* structure, because the energy difference between *cis* and *trans* conformations of HONO is only 1–2 kcal mol^{-1}. The nitro isomer is only 0·6 kcal mol^{-1} higher than the nitrito structure **1** at our best level of theory. This difference is much lower than the energy difference between HONO and HNO_2, about 9 kcal mol^{-1} at the same MP4 level. Thus, replacement of H by C_6H_5 leads to stabilization of the nitro structure. The geometries of the carbon rings are very close in **1** and **4**. Structure **4** is planar, and hydrogen bond-type interactions are possible between the oxygen atoms of NO_2 and hydrogens of the *ortho*-C atoms, with and OH distance of 2.38 Å.

The isomers **2** and **3** with the C(H)(NO) group in *ortho* and *para* positions with respect to the C=O bond, lie 9·9 and 7·2 kcal mol^{-1} higher than **1**. In both cases, the aromaticity of the C_6 ring is destroyed. The ring contains two single C—C bonds, 1·51–1·53 Å, two double bonds, 1·32–1·33 Å and two bonds of intermediate length, 1·47–1·49 Å. The *para*-isomer has C_s symmetry and the C(H)(NO) fragment is located in the mirror plane. The hydrogen and oxygen of this fragment make a weak hydrogen bond, with an OH distance of 2·28 Å. This is not the case for the *ortho*-isomer.

The most stable isomer, **5**, $C_6H_4(OH)(NO)$, has a planar geometry. All CC distances in the aromatic C_6 ring are similar, 1·37–1·40 Å. The NO ligand is located in a *ortho*-position with respect to the OH ligand, and the OH···ON hydrogen bond length is short, 1·88 Å. Other conformations of $C_6H_4(OH)(NO)$, with various mutual locations of the OH and NO ligands, are also expected to be local minima and to have energies similar to that of **5**.

The exothermicity of the reaction

$$C_6H_5O + NO \rightarrow C_6H_5ONO \qquad (6)$$

calculated at the MP4(SDQ)/6–31G* + ZPE level is 10·4 kcal mol^{-1}. However, the approximation used is not reliable enough to describe the energy of the homolytic cleave of the ON bond. Therefore, we use here another approach for calculations of the O—N bond dissociation energy in C_6H_5ONO. The approach involves calculations of heats of formation of C_6H_5O

Table 1. Total (hartree) and relative (kcal mol^{-1}, in brackets) energies and zero-point energy corrections of various isomers of C_6H_5ONO[a]

		E_{rel}[b]			
Species	ZPE[a]	HF	MP2	MP3	MP4(SDQ)
C_6H_5ONO (**1**)	61·1	−434·17769 [17·7]	−435·45026 [12·6]	−435·46346 [15·3]	−435·48402 [12·9]
o-NOC_6H_5O (**2**)	61·1	−434·16616 [24·9]	−435·42073 [31·2]	−435·44560 [26·5]	−435·46832 [22·8]
p-NOC_6H_5O (**3**)	61·1	−434·17285 [20·7]	−435·42441 [28·8]	−435·47257 [20·1]	−435·47257 [20·1]
$C_6H_5NO_2$ (**4**)	62·4	−434·17523 [20·6]	−435·45986 [7·9]	−435·46569 [15·2]	−435·48512 [13·5]
$C_6H_4(OH)(NO)$ (**5**)	61·8	−434·20703 [0·0]	−435·47149 [0·0]	−435·48901 [0·0]	−435·50574 [0·0]
$C_6H_5O + NO$	56·4	−434·22292 [−15·4]	−435·41338 [31·1]	−435·44821 [20·2]	−435·46001 [23·3]

[a] ZPE are calculated at the HF/6–31G* level and scaled by 0·89.

[b] The relative energies are calculated with ZPE (scaled HF/6–31G*).

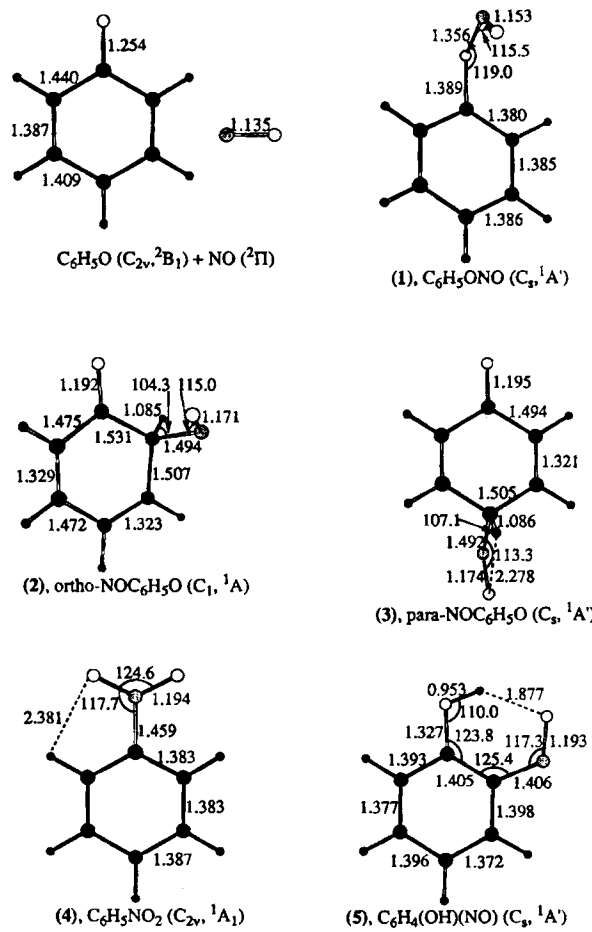

Figure 1. RHF/6–31G* optimized geometries of $C_6H_5N_1O_2$ isomers

and C_6H_5ONO from the isodesmic reactions where the number of bonds of a given type is left unchanged.[20] The reaction for C_6H_5O is

$$C_2H_3O + C_6H_6 \rightarrow C_2H_4 + C_6H_5O \qquad (7)$$

which is calculated to be endothermic by 9·0 and 2·7 kcal mol^{-1} at the UMP4 (SDQ) and spin-projected PUMP3//UHF/6–31G* + ZPE levels of theory, respectively. Because the spin contamination at the UHF and UMPn levels is high for the C_2H_3O and C_6H_5O radicals, as we discussed earlier,[21] the spin-projected PUMP3 energy is expected to be more reliable than the energy calculated by the regular (unprojected) UMP4 (SDQ) method. We use the following heats of formation $\Delta H_f^\circ(0)$ for the species participating in reaction (7): C_2H_3O, 4·8 kcal mol^{-1}, which is derived from the experimental $\Delta H_f^\circ(298)$[22] corrected to 0 K on the basis of calculated HF/6–31G* frequencies; C_6H_6 24·1 kcal mol^{-1}, experimental $\Delta H_f^\circ(298)$[23] corrected to 0 K; C_2H_4, 14·6 kcal mol^{-1}, experimental $\Delta H_f^\circ(0)$.[24] Then, the calculated $\Delta H_f^\circ(0)$ for C_6H_5O is 17·0 kcal mol^{-1}, which is in satisfactory agreement with 15·0 kcal mol^{-1}, the experimental $\Delta H_f^\circ(298)$[23] corrected to 0 K. The reaction for C_6H_5ONO:

$$CH_3ONO + C_6H_5OH \rightarrow CH_3OH + C_6H_5ONO \qquad (8)$$

is endothermic by 7·2 and 7·0 kcal mol^{-1} in the MP3/6–31G* + ZPE and MP4(SDQ)/6–31G* approximation, respectively. For consistency, we use the ΔE, calculated by the MP3 method. (For these closed-shell molecules, the restricted MPn methods, RMP3 and RMP4, were used without spin contamination corrections.) $\Delta H_f^\circ(0)$ for the species involved, derived from the experimental $\Delta H_f^\circ(298)$ values corrected to 0 K, are CH_3ONO −12·6, C_6H_5OH −18·5 and CH_3OH −45·3 kcal mol^{-1}.[23] The calculated $\Delta H_f^\circ(0)$ for C_6H_5ONO is 21·4 kcal mol^{-1}. Using the experimental $\Delta H_f^\circ(0)$ for the NO molecule, 21·5 kcal mol^{-1},[24] one

Table 2. Experimental and calculated (in parentheses) heats of formation of various species

Species	$\Delta H_f^\circ(0)$ (kcal mol^{-1})	$\Delta H_f^\circ(298)$ (kcal mol^{-1})
C_2H_3O	4·8[a]	3·0[b]
C_6H_6	24·1[a]	19·8[c]
C_2H_4	14·6[d]	12·5[d]
C_6H_5O	15·0[a] (17·0)	11·4[c] (13·4)
CH_3ONO	−2·6[a]	−15·8[c]
C_6H_5OH	−18·5[a]	−23·0[c]
CH_3OH	−45·3[a]	−48·1[c]
C_6H_5ONO (1)	(21·4)	(17·1)[e]
o-NOC_6H_5O (2)	(31·3)	(26·8)[e]
p-NOC_6H_5O (3)	(28·6)	(24·0)[e]
$C_6H_5NO_2$ (4)	20·5[a] (22·0)	15·7[c] (17·2)[e]
$C_6H_4(OH)(NO)$ (5)	(8·5)	(4·4)[e]

[a] Calculated on the basis of experimental $\Delta H_f^\circ(298)$ and HF/6–31G* frequencies.
[b] Ref. 22.
[c] Ref. 23.
[d] Ref. 24.
[e] Computed on the basis of calculated $\Delta H_f^\circ(0)$ and HF/6–31G* frequencies.

can calculated exothermicity of the reaction (6) to be 17·1 kcal mol^{-1}, which corresponds to the O—NO bond dissociation energy in C_6H_5ONO.

Experimental and calculated heats of formation of various species are summarized in Table 2. For different isomers of $C_6H_5NO_2$, $\Delta H_f^\circ(0)$ values were calculated from $\Delta H_f^\circ(0)$ of C_6H_5ONO (1) and MP4 (SDQ)//HF/6–31G* + ZPE relative energies. It is worth noting that for C_6H_5O and $C_6H_5NO_2$ (4), where the experimental and theoretical heats of formation can be compared, the discrepancies do not exceed 2 kcal mol^{-1}.

RESULTS AND DISCUSSION

Absorption of C_6H_5O in the visible region

The absorption spectrum of the C_6H_5O radical in the visible region was first reported by Porter and Ward[25] and later in greater detail by Ward.[16] Figure 2 compares Ward's results obtained by flash photolysis–plate photometry with ours acquired by the laser photolysis–CRD absorption method at room temperature. The absorption spectra covering the 550–602 nm spectral region agree qualitatively; they are believed to result from the $\pi \leftarrow$ n transition due to the excitation of a nonbonding p-electron of the O atom to a nonbonding π-orbital of the aromatic system. The fine structures revealed by our laser absorption measurement may represent vibronic bands. Identification of their origins should be feasible through comprehensive and laborious analyses. For kinetic measurement, the laser wavelength was fixed at 575·4 nm throughout the study.

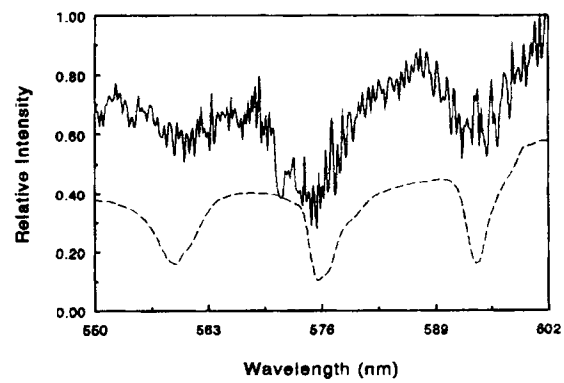

Figure 2. Absorption spectrum of C_6H_5O obtained by photolysis of $C_6H_5OCH_3$ at 193 nm. The dashed curve shows the absorption spectrum of C_6H_5O obtained by Ward;[16] it is shifted for clarity

Kinetics of the C_6H_5O + NO association reaction

The decay of C_6H_5O measured by photon decay times under excess NO conditions, as depicted in Figure 3, was analyzed by the non-linear least-squares method according to equation (5), which can be simplified to

$$1/t_c - 1/t_c^0 = c_1 + c_2 e^{-bt} \quad (9)$$

where $b = k_1[NO] + k_{-1}$. The results presented in Figure 3 clearly show that the decay of the C_6H_5O radical at 297 K is faster and complete, with t_c at long reaction times ($t \rightarrow \infty$) approaching t_c^0, the photon decay time in the absence of C_6H_5O. On the other hand, at 373 K, the decay of C_6H_5O becomes much slower and the absorption at 575.4 nm due to C_6H_5O remains strong at long reaction times.

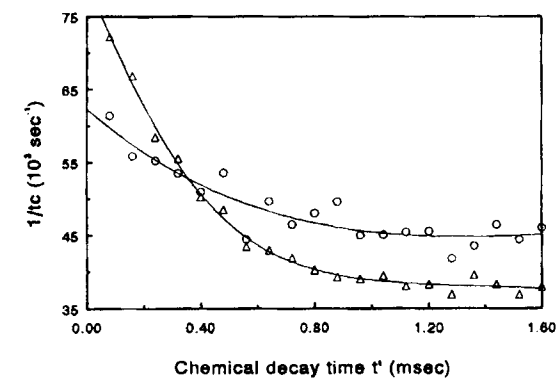

Figure 3. Typical inverse photon decay time plot obtained by the photolysis of $C_6H_5OCH_3$–NO–Ar mixture at 193 nm. The measurements were carried out at (Δ) 297 K with $[NO] = 1·11 \times 1·10^{15}$ molecules cm^{-3} and (○) 373 K with $[NO] = 9·31 \times 10^{14}$ molecules cm^{-3}, respectively. The solid curves are the least-squares fit to equation (9)

Repeating such measurements at different NO concentrations gives varying values of the pseudo-first-order decay constant, $k' \equiv b = k_1[NO] + k_{-1}$, which varies linearly with [NO] as illustrated in Figure 4. The slopes of the k' vs [NO] plots give the bimolecular rate constant for the association reaction

$$C_6H_5O + NO \rightarrow (C_6H_5O)NO$$

The results obtained for five temperatures between 297 and 373 K give $k_1 = 10^{-12\cdot12\pm0\cdot24}e^{(194\pm185)/T}$ cm^3 molecule^{-1} s, where the deviations representing 1 σ were obtained by linear least-squares analysis using the weighting factor $w_i = (k_i/\sigma i)^2$. These results are also presented graphically in Figure 5.

In Figure 5, we have also compared the values of k_1 obtained by equation (1), which assumed no reverse dissociation of the association product, $(C_6H_5O)NO$. The apparent rapid decrease in k_1, or the C_6H_5O decay rate, due to the increased reproduction of the C_6H_5O radical at higher temperatures, resulted in an artificially large negative activation energy for the association process (−4 kcal mol^{-1}). The observed small negative activation energy of 0·38 kcal mol^{-1} for $C_6H_5O + NO$ is close to that of the analogous $C_6H_5 + NO$ reaction,[14] also determined by the CRD method. In the latter case, the redissociation of C_6H_5NO was not detected at temperatures as high as 523 K.

Although the intercepts of the k' vs [NO] plots as given in Figure 4 represent, in principle, the rate constants for the unimolecular dissociation of $(C_6H_5O)NO$; they are not reliable and are effectively useless because of the large scatter of the present data as indicated. Additionally, in the absence of NO, the C_6H_5O radical

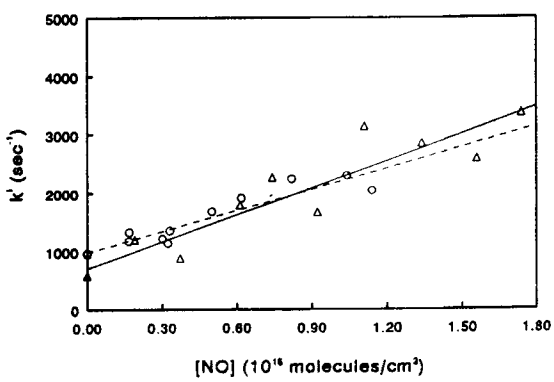

Figure 4. Plots of k' vs [NO] at (Δ) 297 K and (○) 353 K. Linear least-squares fits to these data yield the respective slopes and intercepts: 297K, $(1\cdot53 + 0\cdot21) \times 10^{-12}$ cm^3 molecule^{-1} s) and 703 ± 202 s^{-1}; 353 K, $(1\cdot20 \pm 0\cdot14) \times 10^{-12}$ cm^3 molecule^{-1} s and 985 ± 82 s^{-1}, respectively. The errors represent one standard deviation

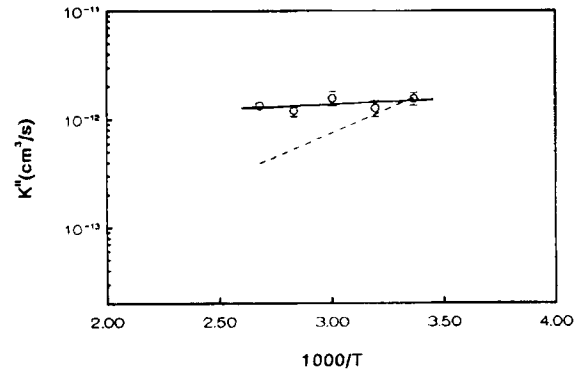

Figure 5. Arrhenius plots of the bimolecular rate constants for $C_6H_5 + NO \rightarrow (C_6H_5O)NO$ from the experiment (40 Torr). The dashed line represents the results evaluated by equation (1). The solid line is the least-squares fit to the results obtained by equation (5), which takes into account the effect of the reverse reaction

may disappear by other side-reactions such as

$$CH_3 + C_6H_5O \rightarrow o\text{-}/p\text{-}CH_3C_6H_4OH$$

$$C_6H_5O + C_6H_5O \rightarrow (C_6H_5O)_2$$

The redissociation of $(C_6H_5O)NO$ during the course of the $C_6H_5O + NO$ reaction above room temperature, as reflected by the kinetic data presented in Figure 3 and 5, is fully consistent with the weak dissociation energies of the association products: 7, 10 and 17 kcal mol^{-1} for o-NOC_6H_5O, p-NOC_6H_5O and C_6H_5ONO, respectively. The O—NO bond in phenyl nitrite is therefore about 25 kcal mol^{-1} weaker[23] than that in methyl nitrite, CH_3ONO, because of the resonance stabilization in C_6H_5O as alluded to in the Introduction. This result is fully consistent with the difference in the bond energies. $D(CH_3O—CH_3) - D(C_6H_5O—CH_3) = 83-57 = 26$ kcal mol^{-1}.[23]

The theoretical molecular parameters (moments of inertia and vibrational frequencies) and heats of formation of C_6H_5O, NO and C_6H_5ONO allow us to calculate the equilibrium constant for the reaction

$$C_6H_5O + NO = C_6H_5ONO$$

to be $1\cdot65 \times 10^{-28}e^{8770/T}$ cm^{3}molecule^{-1} for the temperature range 298–400 K. Combination of this equation with that for k_{-1} given above gives rise to the rate constant for the unimolecular decomposition of C_6H_5ONO: $k_{-1} = 4\cdot6 \times 10^{15}e^{-8580/T}$ s^{-1}. The value of the pre-exponential factor, 4.6×10^{15} s^{-1}, compares closely with that of the CH_3ONO decomposition reaction in the high-pressure limit, $1\cdot0 \times 10^{16}$ s^{-1}.[26] Therefore the transition state of the C_6H_5ONO decomposition reaction is fairly loose.

We also examined the effect of pressure at 333 K by

doubling the total system pressure from 40 to 80 Torr (1 Torr = 133·3 Pa), with no change in the value of k_1 within experimental errors.

CONCLUSION

The kinetics and mechanism for the reaction of C_6H_5O with NO have been studied for the first time by the cavity-ring-down technique. The reaction is believed to occur by direct association forming phenyl nitrite, the most stable isomer of the three likely association products, C_6H_5ONO, *o*-NOC_6H_5O and *p*-NOC_6H_5O, according to the results of our *ab initio* MO calculations. Other more stable isomers, nitrosophenols, could be formed by sigmatropic H-migration, but it is energetically inaccessible in the present case. The bimolecular rate constant for the association reaction has been determined to be $k_1 = 10^{-12\cdot12\pm0\cdot24} e^{(194\pm185)/T}$ cm^3 molecule^{-1} s, with a negative activation of 0·38 kcal mol^{-1}.

On account of the relatively weak C_6H_5O—NO bond energy, as confirmed by the result of MO calculations, the redissociation of C_6H_5ONO was observed to take place above room temperature. The rate constant for the redissociation reaction (k_{-1}) was calculated by means of the measured value of k_1 and the theoretical equilibrium constant: $k_{-1} = 4\cdot6 \times 10^{15} e^{-8580/T}$ s^{-1}. The pre-exponential factor compares reasonably well with that of the methyl nitrite decomposition reaction.

ACKNOWLEDGEMENTS

The authors gratefully acknowledge the support of this work by DOE (contract No. DE-FG05-91ER14192) to T. Yu and by the Office of Naval Research (contract No. N00014-89-J-19490) to A. M. Mebel and M. C. Lin. They also thank the Cherry L. Emerson Center for Scientific Computation for the use of various programs and computing facilities.

REFERENCES

1. I. Glassman, *Combustion*, 2nd ed. Academic Press, New York (1986).
2. A. J. Colussi, F. Zabel and S. W. Benson, *Int. J. Chem. Kinet.* **9**, 161 (1977).
3. C.-Y. Lin and M. C. Lin, *Int. J. Chem. Kinet.* **17**, 1025 (1985).
4. C.-Y. Lin and M. C. Lin, *J. Phys. Chem.* **90**, 425 (1986).
5. A.-M. Schmoltner, D. S. Anex and Y. T. Lee, *J. Phys. Chen.* **96**, 1236 (1992).
6. M. F. R. Mulcahy and D. J. Williams, *Aust. J. Chem.* **18**, 20 (1965).
7. C.-Y. Lin and M. C. Lin, *Aust. J. Chem.* **39**, 723 (1986).
8. J. G. P. Born, PhD Dissertation, Leiden University (1992).
9. A. O'Keefe and D. A. G. Deacon, *Rev. Sci. Instrum.* **59**, 2544 (1988).
10. A. O'Keefe, J. J. Scherer, A. L. Cooksy, R. Sheeks, J. Heath and R. Saykally, *Chem. Phys. Lett.* **172**, 214 (1990).
11. T. Yu and M. C. Lin, *J. Am. Chem. Soc.* **115**, 4371 (1993).
12. M. C. Lin and T. Yu, *Int. J. Chem. Kinet.* **25**, 875 (1993).
13. E. W. Diau, T. Yu, M. A. G. Wagner and M. C. Lin, *J. Phys. Chem.* **98**, 4034 (1994).
14. T. Yu and M. C. Lin, *J. Phys. Chem.* **98**, 2105 (1994).
15. T. Yu and M. C. Lin, *Int. J. Chem. Kinet.* **26**, 771 (1994).
16. B. Ward, *Spectrochim. Acta, Part A* **24**, 813 (1968).
17. For theoretical methods and basis sets, see W. Hehre, L. Radom, P.v.R. Schleyer and J. A. Pople, *Ab Initio Molecular Orbital Theory*. Wiley, New York (1986).
18. (a) S. Nakamura, M. Takahashi, R. Okazaki and K. Morokuma, *J. Am. Chem. Soc.* **109**, 4142 (1987); (b) S. Takane and T. Fueno, *Theor. Chim. Acta* **87**, 431 (1994).
19. M. J. Frisch, G. W. Trucks, M. Head-Gordon, P. M. W. Gill, M. W. Wong, J. B. Foresman, B. G. Johnson, H. B. Schlegel, M. A. Robb, E. S. Reglogle, R. Gomperts, J. L. Andres, J. Raghavachari, J. S. Binkley, C. Gonzales, R. L. Martin, D. J. Fox, D. J. DeFrees, J. Baker, J. J. P. Stewart, J. A. Pople, *GAUSSIAN 92*. Gaussian, Pittsburgh, PA (1992).
20. W. J. Hehre, R. Ditchfield, L. Radom and J. A. Pople, *J. Am. Chem. Soc.* **92**, 4796 (1970).
21. A. M. Mebel and M. C. Lin, *J. Am. Chem. Soc.* **116**, 9577 (1994).
22. G. B. Ellison, P. C. Engelkingl and W. C. Lineberger, *J. Phys. Chem.* **86**, 4873 (1982).
23. D. R. Lide (Ed.), *CRC Handbook of Chemistry and Physics*, 74th ed. CRC Press, Boca Raton, FL (1993).
24. M. W. Chase, Jr, C. A. Davies, J. R. Downey, Jr, D. J. Frurip, M. A. McDonald and A. N. Syverud, *JANAF Thermochemical Tables*, 3rd ed.; *J. Phys. Chem. Ref. Data* **14**, Suppl. 1 (1985).
25. G. Porter and B. Ward, *J. Chim. Phys.* **61**, 1517 (1964).
26. Y. He, W. A. Sanders and M. C. Lin, *J. Phys. Chem.* **92**, 5474 (1988).